Analyzing Gradual Vegetation Changes in the Athabasca Oil Sands Region Using Landsat Data

Moritz Lucas, Antara Dasgupta, and Björn Waske, *Member, IEEE*

***Abstract*—Oil sand mining in northern Alberta/Canada in the Athabasca region is a major intrusion into the otherwise pristine natural environment. The various types of oil sands mining, transport, and processing are causing large-scale discharge of pollutants. Accordingly, this study examined the gradual changes in the physically undisturbed vegetation, that occurred from 1984 to 2021 in the Athabasca oil sands monitoring region. First, the abrupt changes were masked out with the help of auxiliary and Landsat data. Subsequently, a normalized burn ratio Landsat time-series was applied to the LandTrendr algorithm on the Google Earth Engine. In order to interpret gradual changes, measurement criteria were used to describe vegetation development, vulnerability, and variability. In addition, the spatial and temporal relationship of these to oil sand opencast mines, processing facilities, and steam assisted gravity drainage (SAGD) mines was examined. The results showed that a major part of the vegetation in the Athabasca oil sand monitoring region underwent a positive development (65.9%). However, around the opencast mines a negative vegetation development and stability within a radius of 10 km could be observed. In the surroundings of processing facilities, the development and stability of vegetation was disturbed within a radius of 2 km. Thereby the analysis of land cover classes showed that deciduous, coniferous, and mixed forest are disproportionately affected. Conversely, no negative influences on neighboring vegetation could be detected around SAGD mines. The temporal analysis showed that vegetation disturbance was most pronounced between 1990 and 2000, but recovered in recent years.**

***Index Terms*—Forest disturbance, forest recovery, forest monitoring, Google earth engine (GEE), remote sensing, trend analysis.**

I. Introduction

In THE last 50 years, the exploitation of the Athabasca oil sands in Northern Alberta/Canada has increased substantially. Driven by growing global demand for petroleum products and the development of advanced technologies, an extensive industry of extraction, processing, and transportation of oil-related products has grown in the boreal forest [1]. The oil sands at shallow depths are extracted by opencast mining, but in greater depths steam assisted gravity drainage (SAGD) is used [2]. Subsequently, a resource-intensive process takes place to extract the crude oil from the oil sand. This goes hand in hand with extensive land use, high water consumption, and pollution of the surroundings by exhaust gas and leaking tailing ponds [3]. Due to this development and natural factors, vegetation disturbances occur, caused for example by mining, oil processing and transportation, pollution, forest harvesting, urban expansion, wildfires or insect infestations [4].

These can be divided into abrupt, gradual, and seasonal changes [5]. Abrupt changes are mostly due to forest harvesting, mining or urban expansion [6]. Seasonal changes are associated with phenological period of vegetation and can mostly be attributed to climatic changes [7]. Gradual changes, on the other hand, indicate vegetation disturbance due to pollutant input or insect infestation [8]. Most studies of vegetation development tend to focus on abrupt changes [9]. Due to the strong change in spectral reflectance, this is considerably easier to detect. By analyzing gradual changes, disturbances in the vegetation can be detected at an early stage and thus facilitate ecosystem management and nature conservation by allowing preemptive remedial action [8]. Particularly in the Athabasca oil sands region, where the natural environment has been significantly altered, the physically undisturbed part of the vegetation should be monitored, as Canadian Law mandates oil companies to ensure land restoration after use [10]. In this context, there has been plenty of research on the input of pollutants and trace elements from of oil sand mining operations and their impact on the living fauna [11], [12], on rivers and lakes [13], [14], [15], as well as on the surrounding vegetation [16], [17], [18]. Furthermore, the spatial and temporal patterns of trace element deposition using sediment cores were reconstructed [19], [20]. In addition, geographic information systems were used to combine several of these studies and derive spatial structures of the pollutant input [21]. In the field of remote sensing, some studies have already tried to detect these possible gradual vegetation disturbances around the opencast mines in the Athabasca oil sand region. The first focused on land cover change via Landsat and used Advanced Very High Resolution Radiometer from the National Oceanic and Atmospheric Administration (NOAA-AVHRR) to monitor vegetation health [22]. Gillanders et al. researched the land cover development in the immediate vicinity of the opencast mines and could thus determine what kind of vegetation was affected by the mine expansion and will be in the future [23]. Latifovic and Pouliot used Landsat and MODIS data and the normalized difference vegetation index (NDVI) and normalized difference water index (NDWI) to determine gradual changes within the vegetation using linear regression between 1984 and 2012, while using auxiliary data to mask out abrupt changes [24]. In a further analysis, Pouliot and Latifovic in 2016 used temporal segmentation to classify different types

Manuscript received 15 September 2022; revised 14 December 2022; accepted 23 December 2022. Date of publication 6 January 2023; date of current version 24 January 2023. *(Corresponding author: Björn Waske.)*

The authors are with the Institute of Computer Science, Osnabrück University, 49074 Osnabrück, Germany (e-mail: moritzlucas@tutanota.com; antara.dasgupta@uni-osnabrueck.de; bjoern.waske@uos.de).

Digital Object Identifier 10.1109/JSTARS.2023.3234090

of vegetation disturbance and recovery in the vicinity of the opencast oil sand mines [4]. More recent remote sensing studies investigated surface displacement due to SAGD operations [25] and enhanced peatland classification with radar data [26]. Most of these studies focus on the surrounding vegetation of oil sand opencast mines and do not conduct a large-scale monitoring of the entire Athabasca oil sand monitoring (OSM) region. Therefore, little attention has been paid to the effects of other mining methods such as SAGD mines and the effects of processing facilities.

This leads to the following research questions.

1) What gradual changes can be observed in the vegetation within the Athabasca OSM region that has not been influenced by abrupt transformation processes?
2) How do these gradual changes behave in temporal and spatial terms in the vicinity of oil sand opencast mines, processing facilities, and SAGD mines?

Accordingly, the objective of the study is to investigate the gradual changes and trends in vegetation between 1984 and 2021 in the Athabasca OSM region and to examine the spatial and temporal implications of different oil sand mining and processing methods [27].

The following analysis was carried out in the Google Earth Engine (GEE), which provides access to the entire Landsat archive and can improve calculation time through parallel processing [28]. In a first step, the part of the vegetation that underwent an abrupt transformation is masked out with the help of auxiliary data. The Landsat-based detection of trends in disturbance and recovery (LandTrendr) algorithm provided the basis for the investigation of the gradual changes [29]. To describe the gradual changes, the physical quantities velocity, frequency, and variance were calculated to evaluate gradual changes and describe vegetation development, vulnerability, and variability. These results were analyzed within different land cover classes and buffers created around oil sands opencast mines, processing facilities, and SAGD mines. For the temporal investigation, the mean velocity of six-year time periods within these buffers was calculated.

II. Study Area and Data Sets

A. Study Area: The Athabasca Oil Sand Region

The study area is the Athabasca OSM region Fig. 1, which covers an area of 92 885 km^2 in northern Alberta. This is one of four regions of the Oil Sands Monitoring Program established by the governments of Canada and Alberta. The aim of the OSM is to study the environmental impacts of oil sands mining and the effects on indigenous people [27]. The Athabasca OSM region was used as study area, as this region contained different kinds of oil sands mining and large amounts of untouched vegetation. The climate of the site is characterized as subhumid with cold winters and hot summers with long wet and dry periods. The annual average temperature is 1.0 °C and total average precipitation is 418.6 mm [30]. The study area is characterized by boreal forest permeated by wetlands, lakes, and the from south to north crossing Athabasca River [31], [32]. A human footprint can be mainly found in mining activities, urban expansion in the nearby city Fort McMurray and agriculture and logging in the south.

Oil sand is a mixture of bitumen, water quartz sand and clays. Bitumen is a form of heavy crude oil, which have to be extracted from the surrounding soil materials to use it for further products [33]. Shallow oil sand can be mined by opencast mining and extracted by mixing the oil sand with hot water using natural gas [34]. However, two thirds of the deposits are too deep to mine it from the surface and thus, the SAGD technology is used [2]. Here, natural gas is mixed with water to produce steam, which is pumped into the deep-seated oil sand deposits [35]. Therefore, the viscosity of the oil sand is increased, which is then plumbed to the surface by production wells [3]. The different deposits can be seen in Fig. 1, where the dominance of SAGD technology is evident.

B. Data Collection

Annual surface reflectance composites were produced for the period between 1984 and 2021 using Landsat TM/ ETM+/ OLI, which provided a continuous resolution dataset of land surface observations of 30 m to date. For this purpose, USGS Landsat surface reflectance Level 2 Collection 2 Tier 1 datasets were selected, which have already undergone atmospheric and geometric correction. For each year all available data between June and September was used (see Sections III-A and III-B). This period represents the main growing season and therefore, it is likely that the spectral contrast between stable forest patches and gradual vegetation changes is highest. The Human Footprint Inventory 2019 enhanced for OSM Region (HFI) and Historical Wildfire Perimeter Data: 1931–2020 (HWP) are the basis for masking abrupt changes (see Section III-C). The HFI consolidates 21 human footprint categories, based on more than 115 anthropogenic disturbance types, into a single integrated dataset. It was created by intersecting various data (e.g., infrastructure data), by thematic mapping based on SPOT 6 satellite imagery from 2017 to 2019 [36]. The HWP provide shapefiles about the extent of wildfires from 1931 to 2020, here only the data from 1970 onwards was used, as the areas further in the past have already gone through extensive regeneration [37]. Data extracted from the HFI were also used to analyze the spatial and temporal relationships between vegetation changes and oil mining and processing methods. In order to compare the results on different land cover classes, the forest land cover maps of Hermosilla et al. from 2019 were used [38]. From the OSM Regions dataset, the Athabasca region was selected as the study area. Derived out of the Oil Sands Project Boundaries available between 1985 and 2015, the most recent data was used, to provide an overview of the spatial distribution of different types of oil sand mining in Fig. 1. Table I summarizes the data used herein.

III. Methods

A. Data Preprocessing

Annual Landsat composites were generated between 1984 and 2021. To harmonize differences in spectral characteristics between ETM+, TM and OLI, the OLI image bands 2, 3, 4, 5, 6, and 7 were transformed to the spectral properties of ETM+ bands 1, 2, 3, 4, 5, and 7, respectively, using slopes and intercepts from reduced major axis regressions reported in Roy et al.

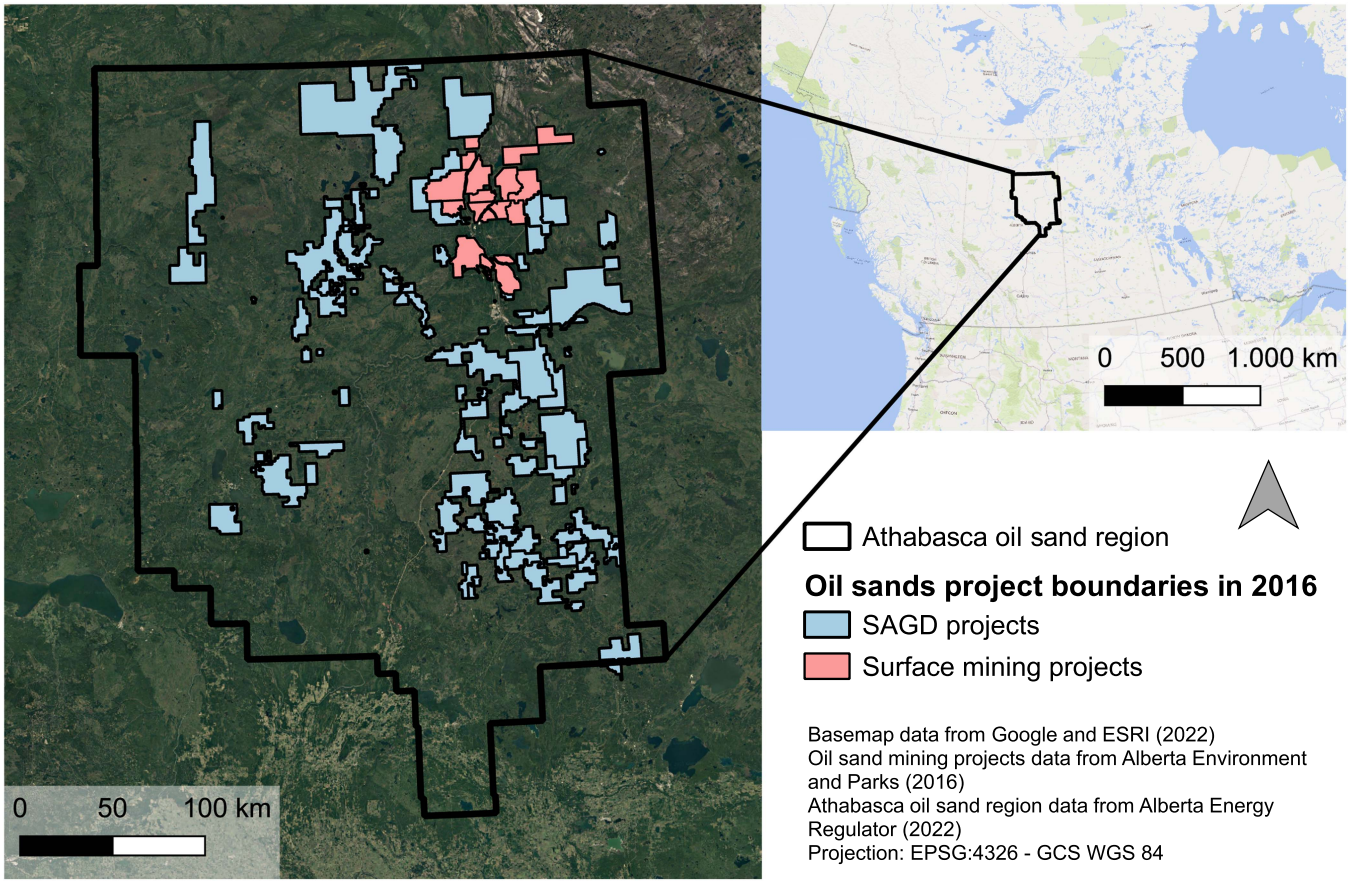

Fig. 1. Map showing the study area formed by the Athabasca oil sand region, the oil sand mining project boundaries, and their location in North America.

TABLE I
DATASETS USED IN THE STUDY, THEIR DESCRIPTION, USAGE AND SOURCES

Data	Description	Usage	Data Sources
Landsat (TM, ETM+, OLI)	Collection of annual atmospheric corrected surface reflectance from June to September 1984–2021	Preparation of annual NBR and NDVI collections as input for LandTrendr and vegetation masking	Surface reflectivity Tier 1 dataset available from GEE
Human Footprint Inventory 2019 Enhanced for OSM Region (HFI)	Information about all areas in OSM Athabasca region that are impacted by human activities	Masking abrupt changes caused by human influence and data source for spatial and temporal analysis of gradual changes	Alberta Biodiversity Monitoring Institute
Historical Wildfire Perimeter Data: 1931–2020 (HWP)	Shapefiles which describe the borders of historical wildfires in Alberta	Masking abrupt changes caused by wildfires	Alberta Agriculture and Forestry
OSM Regions	Regions for monitoring oil sands environmental impact used for forming the study area	Selecting the study area	Alberta Energy Regulator
Oil Sands Project Boundaries 1985 to 2015	All oil sand project boundaries by kind, year and company. Here are only the most recent used	Used in Fig. 1 to provide an overview about the spatial distribution of types of oil sand mining	Alberta Environment and Parks
Land cover 1984–2019 Version 2	High-resolution annual forest land cover maps for Canada's forested ecosystems (1984–2019)	Set NDVI threshold and analyzing measurement criteria	National Forest Information System

Abbreviations: TM=Thematic Mapper, ETM+=Enhanced Thematic Mapper, OLI=Operational Land Imager, NBR=Normalized Burn Ratio, NDVI=Normalized Differential Vegetation Index, GEE=Google Earth Engine, OSM=Oil Sand Monitoring.

Table II [39]. Afterward, CFMASK was applied to mask cloud, cloud shadows, snow, and water [40]. All data of a year were taken to create a composite, conducted by using the median of each spectral value [24]. Then, spectral indices were calculated, which were input for the LandTrendr algorithm and for the vegetation mask described below Fig. 2(a).

To ensure that only areas that were covered with vegetation during the study period were included in the analysis, a vegetation mask was created. For this, an NDVI threshold was defined that separates vegetation from nonvegetated areas, a widely used method to measure relative vegetation abundance [41]. Therefore, a median NDVI composite was formed in 2019 between

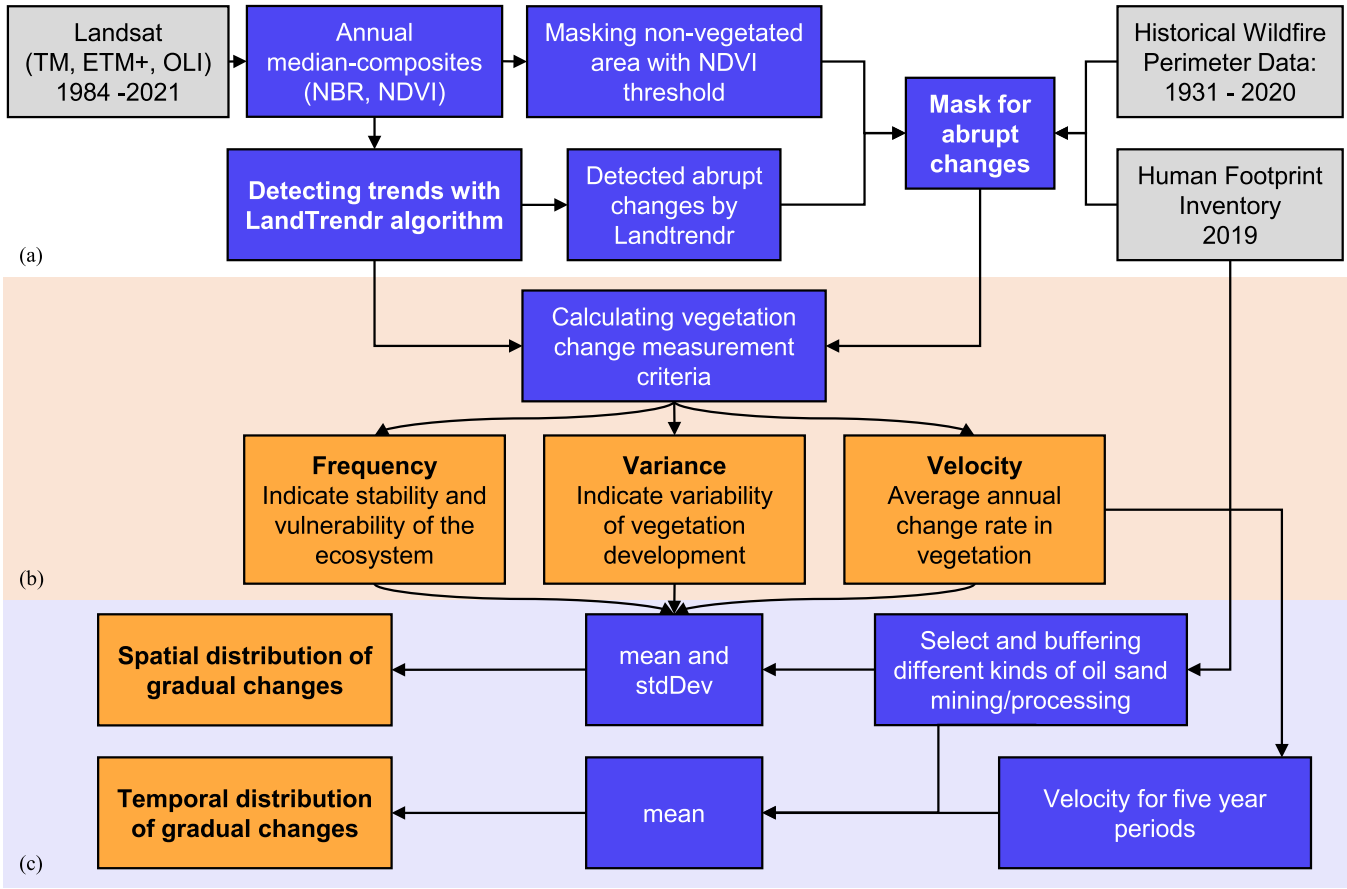

Fig. 2. Flow chart of the methods used in this study to detect the spatial and temporal distribution of gradual vegetation changes in Athabasca OSM region. Segments (a) II-B III-A III-B III-C, (b) III-D, and (c) III-E are used to refer to them at appropriate Sections in the text.

TABLE II
MEASUREMENT CRITERIA USED IN THE STUDY AND THEIR INTERPRETATION IN TERMS OF VEGETATION DEVELOPMENT

Measurement criteria	Interpretation
Velocity V	Average annual change rate in vegetation. Negative values indicate a loss of vegetation, while positive values an additional gain.
Frequency F	Low values indicate stability and high values vulnerability of the ecosystem.
Variance S	The greater S is, the greater is the variability of vegetation development.

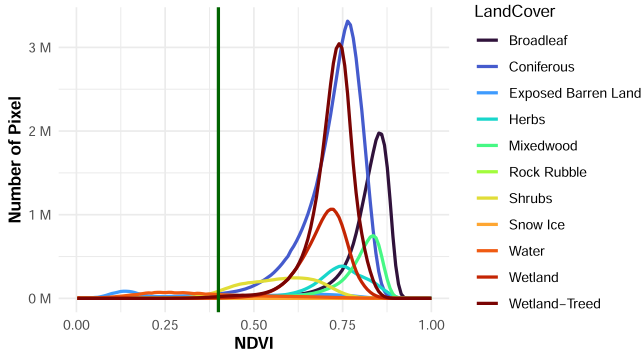

Fig. 3. Histogram of NDVI values corresponding to land cover classes according to Hermosilla et al. [38]. The vertical line represents the NDVI threshold.

June and September and then intersected using the land cover product of Hermosilla et al. also from 2019 [38]. The resulting histogram is shown in Fig. 3. Based on this, the threshold value for vegetation masking was set to 0.4 in order to include all vegetation classes in the analysis. Accordingly, all areas that fell below this value between 1984 and 2021 were masked out, and the resulting masks were merged Fig. 2(a).

B. Change Algorithm and Spectral Disturbance Index

The LandTrendr algorithm was selected as change algorithm to detect gradual changes within the time series. The algorithm has been developed for application to forest disturbances and has since become one of the most widely used algorithms for the detection of abrupt and gradual forest changes [42]. In addition, the implementation in GEE enables processing large amounts of data lending scalability [29].

LandTrendr is a temporal segmentation algorithm based on a yearly time series of spectral indices, to capture both gradual and abrupt changes. It simplifies the time series using a model and detects as breakpoints inflection points in the curve, where the current trend reverses or intensifies. The trends are identified using linear regression, reducing noise by smoothing out outliers without losing significant amounts of detail. At the breakpoints, a temporal segment ends and a new one begins. The algorithm

outputs include a linear regression model fitted to the spectral data and the detected breakpoints [42]. Since there were no *in situ* data in which the fitted models could be compared with ground truth, the parameters were left at the default settings.

A Landsat time series of the normalized burn ratio (NBR) was used as an input for the LandTrendr algorithm Fig. 2(a). NBR is the normalized ratio between near-infrared and short-wave infrared (SWIR) bands. The possibilities to characterize forest structures with SWIR wavelengths are well understood [43]. Kennedy et al. showed that the NBR was most effective spectral index to detect forest disturbances in Landsat time series [42], [44], due to the high sensitivity toward moisture [45]. Despite the moisture sensitivity being an asset for understanding vegetation disturbance, changes in soil moisture could influence the estimates of vegetation development. However, areas with a high proportion of bare soil and outliers in terms of annual wetness were masked out, we expect the influence on the quantitative vegetation development estimates to be minimal.

C. Masking Areas Under Influence of Humans or Natural Disasters

After masking out the nonvegetated areas, only those vegetated pixels should be part of the analysis that is not affected by human-induced changes or natural disasters. For this purpose, the following areas were, thus, masked out

1) Areas under direct human influence.
2) Former wildfire areas, which show afterwards a strong positive vegetation development caused by regeneration.
3) Other areas that are suffering abrupt changes, e.g., windthrow.

Pipeline right of way, seismic lines, access roads, and other oil and gas footprints going through the reclamation process may also have vegetation (likely herbs and bryoids). However, these obviously do not mean actual vegetation regeneration and should not contribute to the present analysis. Accordingly, all human influenced areas were masked out *a priori* using the HFI. To mask out former wildfires in the study area the HWP were used Fig. 2(a). In order to identify further areas with abrupt changes, only changes that lasted one year and exceeded a certain magnitude of change were detected by the LandTrendr algorithm. Therefore, a threshold value t had to be determined. For this purpose, the d_{NBR} was introduced, which represents the difference in the NBR in two consecutive years. Then, 1000 sample points were randomly selected and the mean m and standard deviation std of the d_{NBR} over all years of the study period at these points were used to calculate the threshold value

$$t = m + 2 * \text{std}. \tag{1}$$

All vegetation losses within a year that were greater than this threshold were not included in the analysis [46]. Vegetation regeneration did not have to be considered in this case, as it cannot occur at such a fast rate and is therefore smoothed by the LandTrendr [42]. All resulting masks were combined and provided the basis for the following steps.

D. Analyzing Vegetation Changes

In order to evaluate gradual changes in the ecosystem, an approach of Ye et al. was adapted and modified [9]. There, the use of physical terms Velocity V, Frequency F, and Variance S was proposed for the description of vegetation change measurement criteria Fig. 2(b). In this article, the calculation and use of V in particular is expanded and changed from the original approach. In addition, a spatial and temporal investigation is carried out with regard to different types of oil sand mining and extraction.

The measured value of V describes the average annual rate of change in vegetation. Negative values indicate a loss of vegetation, while positive values signify an additional gain. In order to get an overview of the changes over time, changes were calculated in six-year periods (first and last period include seven years) by using the fitted LandTrendr data [47]. In the following, an average over the entire study period was formed from these sections

$$V_1 = \frac{\text{fit}_{1990} - \text{fit}_{1984}}{t_1} \quad \ldots \quad V_7 = \frac{\text{fit}_{2021} - \text{fit}_{2015}}{t_7} \tag{2}$$

$$V = \frac{\sum_{i=1}^{7} V_i}{7} \tag{3}$$

where V_1 to V_7 are the average annual change rate in vegetation in one period, fit_{year} is the fitted LandTrendr data of the displayed year, t_1 to t_7 are the time in years for the respective period and V is average over all periods. To simplify interpretation, the result was reclassified into four levels:

$$loss \leq -2, weak\ loss \leq 0, weak\ gain \leq 2 \text{ and } gain > 2$$

The measurement criterion F describes the stability or vulnerability of the ecosystem. Low values indicate stability and high values vulnerability [48]. This is derived from the number of fitted segments generated by the LandTrendr algorithm. These can show a positive or a negative development. The results will include the total number, number of positive, and negative segments in the investigation period. A positive segment can be interpreted as a period of regeneration and a negative segment as a period of disturbance.

The measurement criterion S describes the variability of vegetation development, where high values indicate high variability. This is derived from the variance of the time series. S is calculated as follows:

$$S = \frac{\sum_{i=1}^{n} (x_i - \overline{x})^2}{n - 1} \tag{4}$$

where x_i represents the source data in a pixel in year i, $\overline{x_i}$ represents the mean in year i and n represents the number of years in the investigation period. In order to understand the type of vegetation regeneration within the vicinity of the mining sites, the land cover product of Hermosilla et al. [38] was used to calculate a histogram of the respective values. Only five classes were used (Broadleaf, Coniferous, Mixedwood, Wetland, Wetland-Treed), as the others only covered a negligible area within the study region.

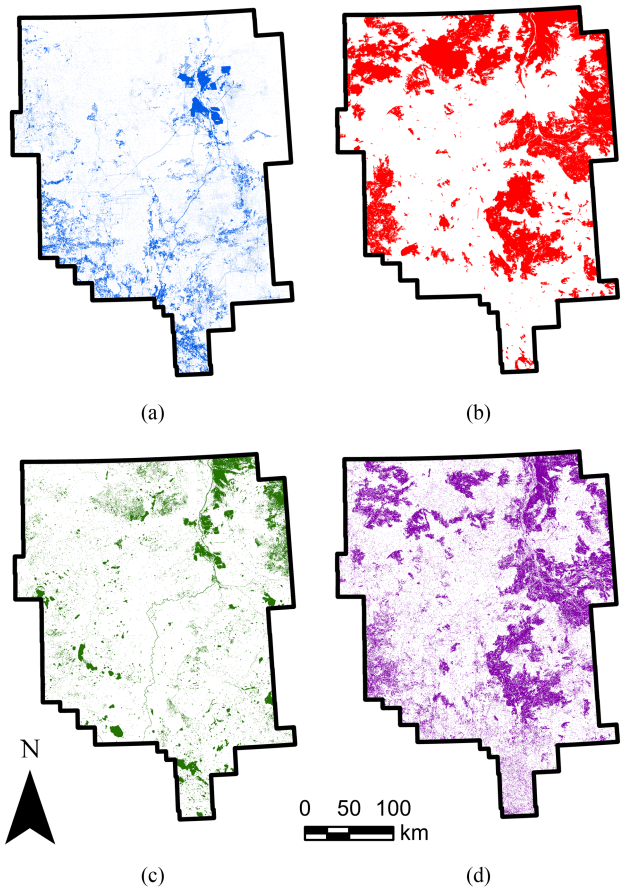

Fig. 4. Spatial distribution of the different masked areas. (a) by Human Footprint Inventory 2019 enhanced for OSM Region (HFI) (b) by Historical Wildfire Perimeter Data: 1931–2020 (HWP) (c) by NDVI threshold (d) of abrupt changes detected by the LandTrendr algorithm. (a) HFI 2019. (b) HWP 1970–2021. (c) Non-vegetated area. (d) Abrupt changes.

E. Spatial and Temporal Distribution of Gradual Changes

In order to analyze the spatial and temporal distribution of the described measurement criteria and to understand the impacts on the vegetation, the surroundings of oil sands opencast mines, processing facilities and SAGD mines were evaluated Fig. 2(c). The data basis is formed by the HFI; this consists of shapefiles where the attribute *FEATURE_TY* indicate the anthropogenic disturbance type. For the opencast mines, the attributes *MINES-OILSANDS*, *TAILING-POND,* and *RIS-MINING-OILSANDS* were selected, what corresponds to areas with bare and/or low vegetated ground and low human density for the purpose of oil sands mining and tailings ponds. In place of oil processing facilities, the attribute *OIL-GAS-PLANT* [36] was selected, under which different industrial sites used for oil production were summarized. For SAGD mines, the attribute *WELL-BIT* was selected, what represents bitumen well pads. The shapefiles were checked for correctness by visual interpretation using satellite images from Google Earth. To quantify the spatial distribution buffers of different sizes (0.25 km, 0.5 km, 1 km, 2 km, 3 km, 4 km, 5 km, 10 km) were used and afterwards the mean and the standard deviation (stdDev) of the measurement criteria of all underlying pixels were calculated. Further, to examine the temporal distribution of the gradual change, the mean of the measurement criteria V of all pixels inside the buffer within the six-year periods were calculated.

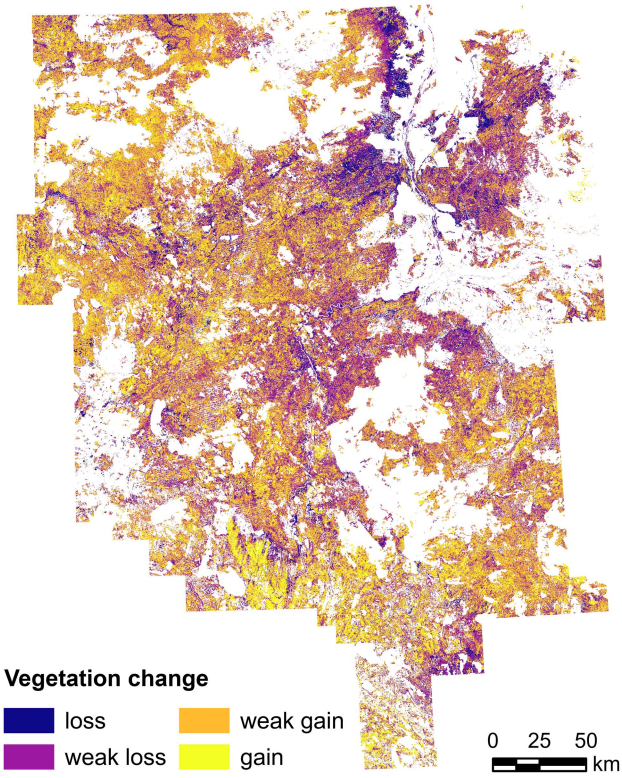

Fig. 5. Average annual vegetation change Velocity (V) between 1984 and 2021.

F. Distribution of Abrupt Changes

By masking out areas under human influence, previous wildfire areas, nonvegetated areas and areas undergoing abrupt changes, an area of 51 766 km^2 was excluded from the analysis. Fig. 4 shows the distribution of the different masks used. The mask of forest fires Fig. 4(b) demonstrate the greatest extent, particularly evident in the peripheral areas in the north, east, and west. In addition, there is the mask of human impact Fig. 4(a), which is dominant in the north-east. The nonvegetated and abrupt changes mask Fig. 4(c) and (d) mostly coincide with the previously mentioned ones. The nonmasked area of 41 119 km^2, which is subsequently analyzed, is mainly located in the center of the study area.

IV. Results

Hereafter, the results of the analysis of the measurement criteria Velocity (V), Frequency (F), and Variance (S) are described. Afterward, the characterisation of the spatial and temporal distribution of gradual changes is presented.

A. Analyzing Annual Change Rate

The velocity (V) was used to describe the average annual vegetation change over the past 37 years. The spatial and temporal distribution of V is shown in Figs. 5 and 6. The spatial distribution of V is presented in Fig. 5, which shows that the

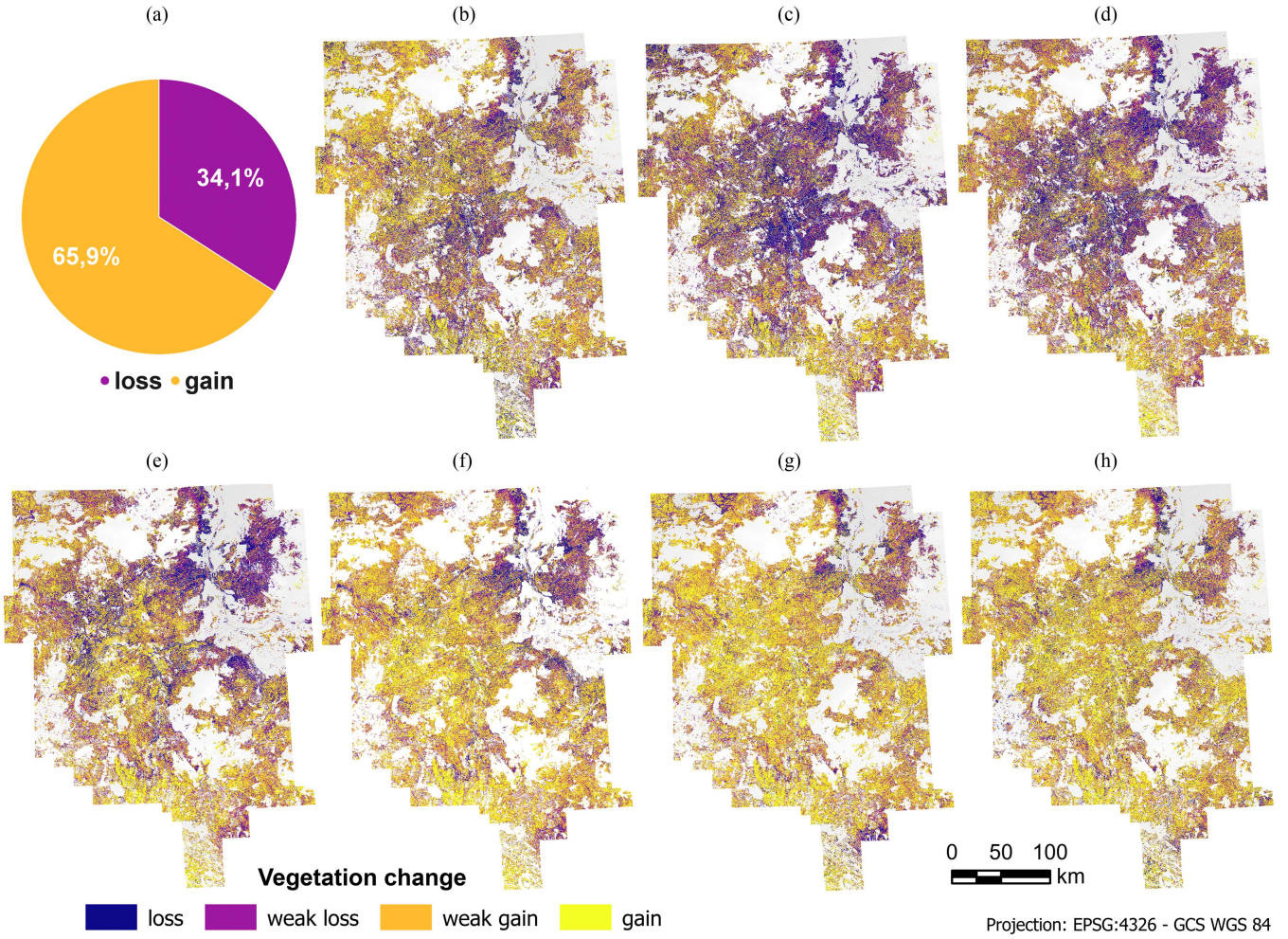

Fig. 6. Average annual vegetation change Velocity (V): (a) V between 1984 and 2021 (b) Histogram of V between 1984 and 2021 (c) Total share of loss and gain in vegetation 1984 and 2021 (d)–(j) V in the specified period. (a) 1984–2021. (b) 1984–1990. (c) 1990–1995. (d) 1995–2000. (e) 2000–2005. (f) 2005–2010. (g) 2010–2015. (h) 2015–2021.

negative trends are particularly concentrated in the north-eastern part around the opencast mines. In contrast, positive trends dominate in the western and southern parts. The proportion of positive and negative vegetation changes over the entire study period can be seen in Fig. 6(a). While positive changes clearly dominate (65.9%), a substantially smaller proportion (34.1%) showed a negative trend. A clear trend can be observed in the temporal distribution of V in Fig. 6 parts b to h. From 1984 to 2000, negative trends increased, especially in the center and north-east of the study area. From 2000 onward, this trend was reversed, especially in the center of the study area. It is noteworthy that negative trends continue to persist in the north-east.

Fig. 7 shows how V behaves within different land cover classes, and a large proportion of the study site does exhibit a positive trend. Furthermore, it is evident that the majority of the Wetland-Treed, Wetland, and Coniferous classes are subject to a positive trend, with the Coniferous class showing the least positive trend. The Broadleaf class experienced no particular trend, while the majority of the Mixedwood class shows a negative trend.

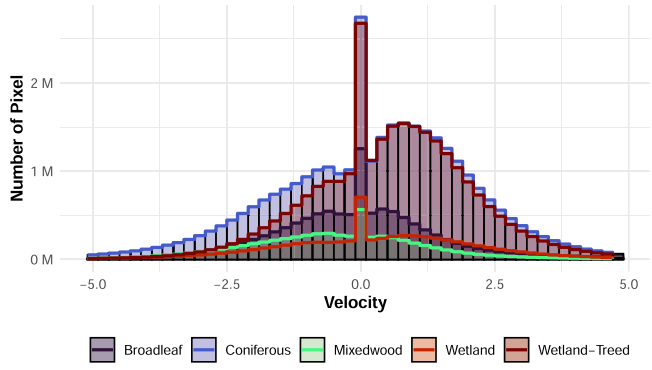

Fig. 7. Histogram of average annual vegetation change Velocity (V) calculated from 1984 to 2021 within different forest land cover classes.

B. Analyzing Stability and Vulnerability

The Frequency (F) is an indicator for the stability and vulnerability of the vegetation Fig. 8. Here, low values represent the stability and high values vulnerability of the ecosystem, which is derived form the number of fitted segments by the LandTrendr

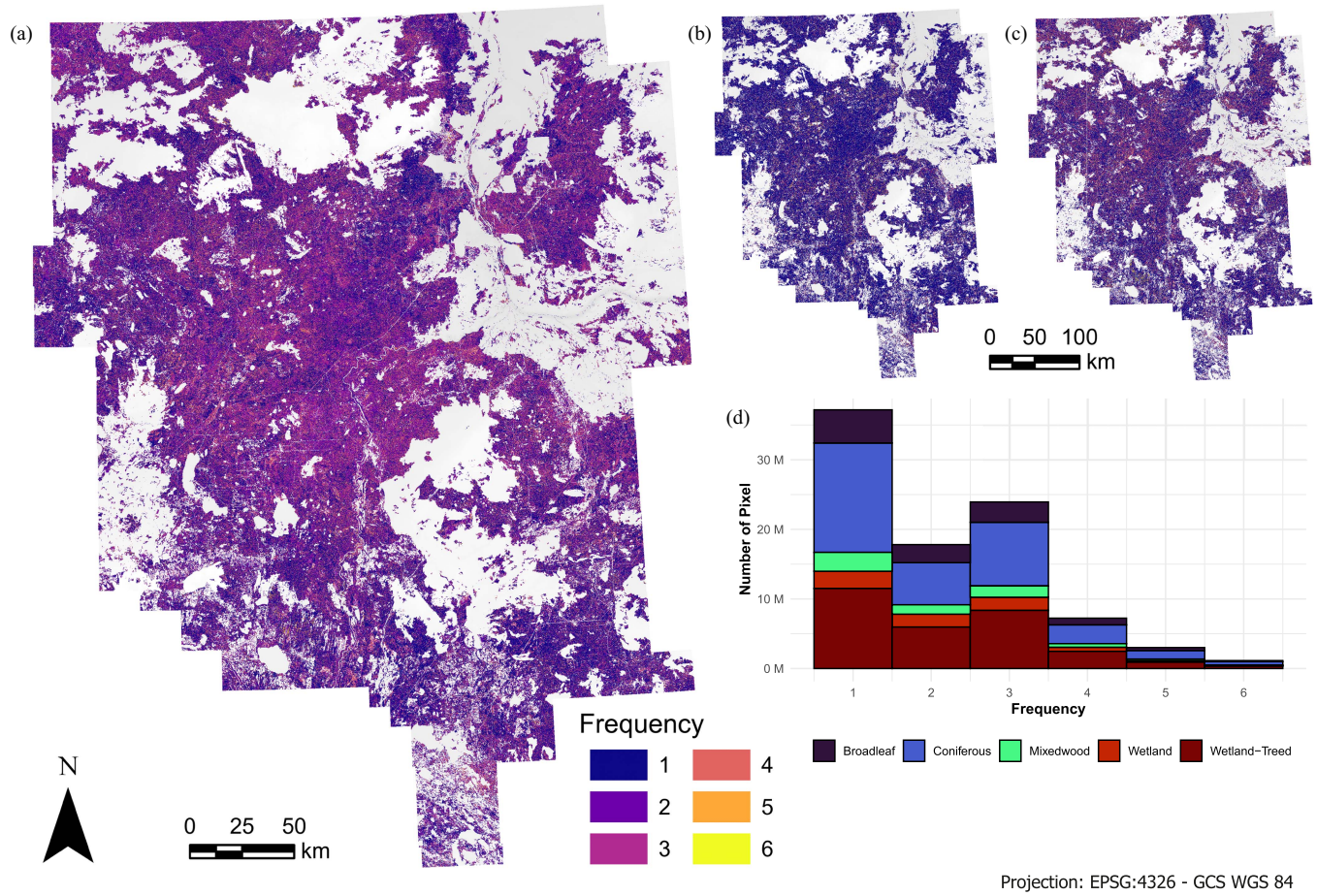

Fig. 8. Number of fitted segments by LandTrendr Frequency (F), with a map in (a) showing all segments, in (b) showing loss segments, and in (c) the gain segments. Histogram (d) [corresponding to a] shows the stacked number of all segments within land cover classes.

algorithm. An overview of the spatial distribution of the number of all segments is given in Fig. 8(a). Fig. 8(d) provides the corresponding histogram. A large part of the area is characterized by low F values. Moreover, the spatial distribution does not show any visible trends, except for minor local variations. The number of segments broken down by loss and gain is shown in Fig. 8(b) and (c). It can be observed that a considerable amount of the pixels contain only one loss segment, whereas the amount of pixels containing two or more gain segments is substantially higher. Fig. 8(d) shows that most of the pixels contain one segment, then the number of pixels decreases with each further segment, with the exception of three segments, where an increase can be seen. Fig. 8(d) shows also the number of pixels per land cover class, whereby it becomes evident that the Coniferous, Wetland-Treed, and Broadleaf classes has a disproportionate number of pixels with three segments.

C. Analyzing Variability

The variance (S), where high values refer to a larger variability in the vegetation development, is depicted in Fig. 9. The spatial distribution of S in Fig. 9(a) shows that the majority of the study area is dominated by low S, interspersed with isolated areas of high S. High S is remarkably frequent in the center, south and north-east around the opencast mines. These observations can be confirmed by the variance within land cover classes in Fig. 9(b): A small part shows values close to zero S, while the majority of pixels exhibit low S, followed by monotonically decreasing number of pixels with increasing S. There are no noticeable differences between the classes, except for the wetland class, which shows a much later increase and therefore a higher overall variance value.

D. Spatial Distribution of Gradual Changes

The spatial distribution of the measurement criteria V, F, and S is represented by the mean and standard deviation within buffers around the oil sand opencast mines, processing facilities and SAGD mines is shown in Fig. 10. Within V Fig. 10(a), a positive dependency of proximity can be observed for opencast mines and processing facilities; this is clearly more pronounced for opencast mines and the negative influence persists up to a distance of 10 km, while for processing facilities a negative dependency can only be seen up to a distance of 2 km. In the case of SAGD mines, a negative dependency is visible up to a distance of 1 km. There seems to exist no dependency between

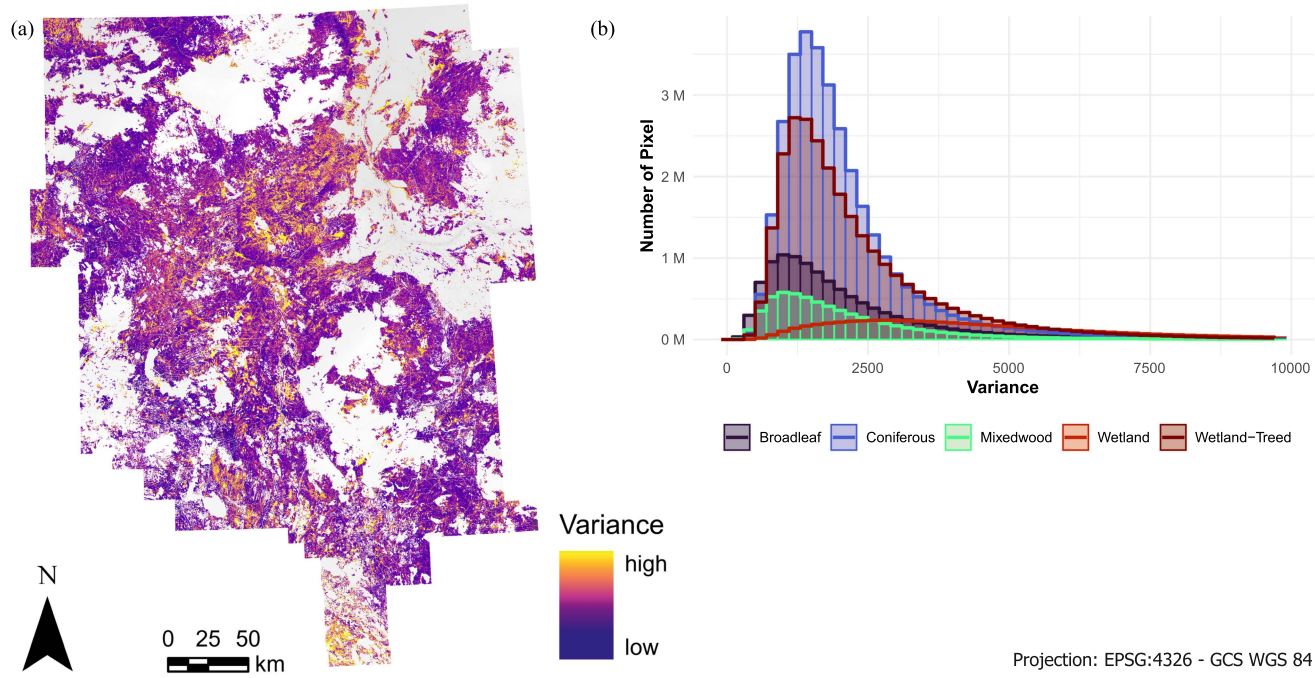

Fig. 9. Variance (S) of the time series summarized in (a) as the spatial distribution of S and in (b) as the histogram of variance within different land cover classes.

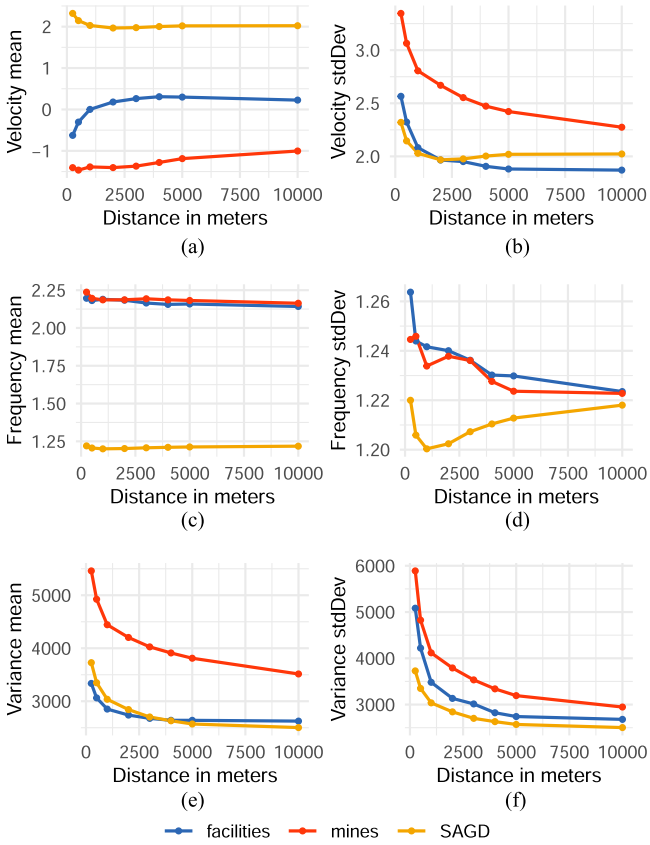

Fig. 10. Mean and stdDev of the measurement criteria of (a) Velocity, (b) Frequency and (c) Variance in the surrounding of oil sand opencast mines, processing facilities and SAGD mines. (a) Velocity mean. (b) Velocity stdDev. (c) Frequency mean. (d) Frequency stdDev. (e) Variance mean. (f) Variance stdDev.

proximity and the development of F Fig. 10(c), but it is striking that F is considerably lower in the vicinity of SAGD mines than at processing facilities and opencast mines. S shows a negative dependence of proximity for opencast mines Fig. 10(e), processing facilities and SAGD mines. The negative dependency is most pronounced for opencast mines. The stdDev shows a decline with increasing distance in all cases Fig. 10(b), (d), and (f). Here, opencast mines show the highest stdDev followed by processing facilities and SAGD mines.

E. Temporal Distribution of Gradual Changes

The temporal distribution of gradual changes in the surroundings of oil sand opencast mines, processing facilities, and SAGD mines is shown in Fig. 11. In the vicinity of the opencast mines Fig. 11(a), the development of enveloping vegetation is consistently negative between 1990 to 2010, although a slight positive dependency can be observed, which is particularly strong between 1990 and 2000 at short distances. The periods from 1984 to 1990 and from 2010 to 2021 show a positive vegetation development, but no specific dependence. In the vicinity of processing facilities Fig. 11(b) a negative vegetation development from 1990 to 2005 and a mostly positive development in the remaining time periods can be observed. The strong positive dependence within short distances is striking for several time periods. In the vicinity of SAGD mines Fig. 11(c), only the periods from 1990 to 2000 showed a negative development; in all other periods, the development was mostly positive. Overall, there is no dominant dependency; both slightly positive and negative trends could be identified. A strong positive dependence in the period from 1995 to 2000 is clearly visible.

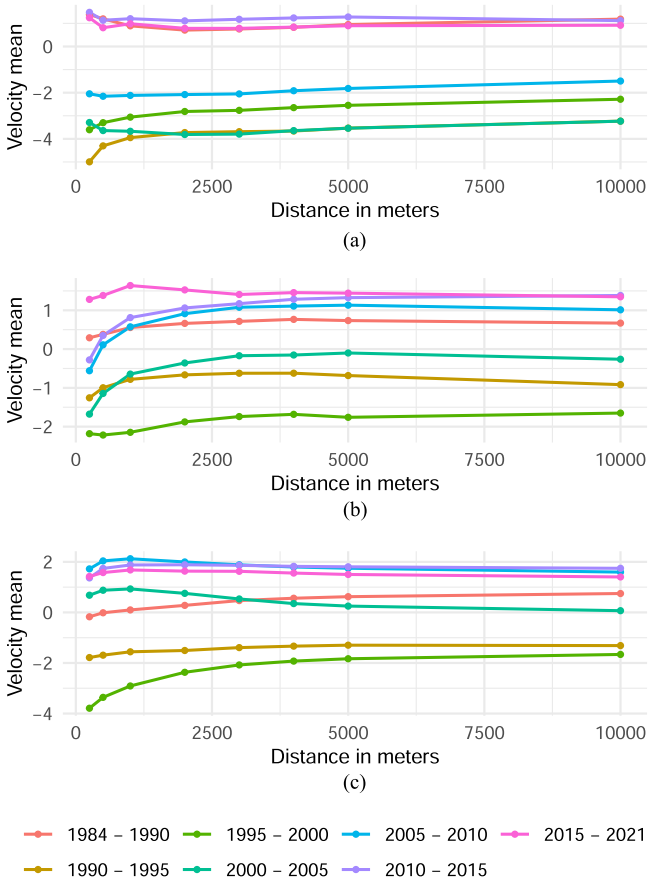

Fig. 11. Mean of Velocity within buffers of (a) oil sand opencast mines, (b) oil processing facilities and (c) SAGD mines of different time periods. (a) Mines. (b) Facilities. (c) SAGD.

V. Discussion

In this study, gradual changes in physically undisturbed vegetation were identified using LandTrendr algorithm and measurement criteria V, F, and S. To achieve this, abrupt changes were masked out using different approaches. The most prevailing abrupt changes were forest fires and mining activities. Similar results for abrupt changes were obtained by Pouliot and Latifovic in 2016, where the gradual changes showed that insect infestations played an important role [4]. Gradual changes can also increase with stress from forest disturbance due to clearing and expansion of industrial activities [4]. As these could not be masked out due to the lack of *in situ* data, insect infestation may therefore be part of the gradual changes detected in this study. Another unnoticed aspect that influences the gradual changes is climate. The climate normalization of a gradual trend analysis of the vegetation by Latifovic and Pouliot in 2014 showed that the climate or climate change only slightly influences gradual changes [24].

The investigation of V showed that the vegetation in undisturbed parts of the Athabasca OSM was largely subject to a positive development, although it must be acknowledged that some of this detected regeneration may have been contributed by invasive species. However, as satellite imagery from Landsat was used here, and it was not possible to get corresponding high spectral or spatial resolution data, the specific contribution of invasive species could not be estimated [49], [50]. The detected negative development was spatially concentrated in the area around opencast mines in the northeast, which was additionally confirmed by the spatial investigation carried out in Section IV-D. These demonstrated a negative influence on vegetation up to a distance of 10 km and beyond. It also showed that processing facilities have a negative impact on the surrounding vegetation at distances of up to 2 km, whereby the analysis of the land cover classes showed a disproportionate impact on deciduous, coniferous, and mixed forest. Conversely, no negative influence could be detected in the vegetation surrounding SAGD mines using the methods proposed herein. One of the reasons for this could be that land disturbances from SAGD mining are typically observed off-site and vegetation impacts are likely displaced upstream (see [51] for further details). As only the vegetation changes in the immediate vicinity of mining sites was investigated herein, the upstream and off-site vegetation disturbances could not be quantified. These observations were further supported by the measurement criteria of F and S, which indicate variability and stability of vegetation development. No dependence between proximity and the value of F was found, but it is worth noting that both the surroundings of opencast mines and processing facilities showed substantially higher values and thus weaker stability in the vegetation than SAGD mines. On the other hand, S decreased with increasing distance in all studied areas; this could be attributed to a smoothing effect with a larger amount of pixels within larger buffers. SAGD mines and processing facilities showed a very similar development, while opencast mines showed a notably higher value of S. In summary a negative vegetation development prevailed in the vicinity of opencast mines and that this was accompanied by high variability and unstable vegetation. Similar results in vicinity to opencast mines were also observed by Latifovic et al. [22] and by Latifovic and Pouliot [24]. Indeed, it would be valuable to validate the results, even if only for a small part of the study area, but unfortunately, no suitable datasets could be found. In future, however, curating field-based and high-resolution (e.g., drone/aerial photography) vegetation regeneration observations could help validate such studies, contributing to the development of satellite-based systematic vegetation monitoring systems. In relation to the negative vegetation development around the opencast mines and processing facilities, numerous studies have investigated the impact of atmospheric deposition of acid [16], [17], [52], polycyclic aromatic hydrocarbons (PAHs) [53], [54] or trace metals [19], [20] emitted by oil sand mining and processing in the surrounding vegetation. These are mostly released into the environment by dust particles and increased concentrations are related to the vicinity to opencast mines and lead to an impact on vegetation growth and species distribution [13], [55]. Another factor is contamination of the surrounding water system. For example, large quantities of mostly toxic trace metals emitted during the oil sand processing are released into the rivers during the snow melt [14], [34].

It has also been identified that the tailing ponds, which are supposed to absorb incoming waste water, are leaking it into the groundwater [56]. Furthermore, the impact of oil sands mining on the climatic conditions in the vicinity of open pit oil sands mining was also investigated, revealing that the average temperature increased by 1.2 °C compared to the regional average [57]. This combination of trace metals, PAHs, contaminated water and changes in the regional climate could have led to the negative impacts found around opencast mines and processing facilities. Ground movement (heave/subsidence) due to SAGD operations could also impact the spatial and temporal distribution of vegetation changes. However, as the heave and subsidence is limited to a few centimetres per year and stop after a few years [58], [59], it has been assumed that this has limited influence on the vegetation. Indeed, this also presents an interesting opportunity for future research, although it is out of scope for this particular study.

The temporal development of V in Sections IV-A and IV-E showed that between 1990 and 2000, the majority of the vegetation in the study area underwent a negative development. The periods from 1984 to 1990 and from 2010 to 2021, on the other hand, clearly showed a positive vegetation development. In the period from 1984 to 1990, this can be explained by more distant mining activity, which has steadily expanded since then. However, the regeneration of vegetation development in the period from 2010 to 2021, could be attributed to improvements to mining and upgrading technologies, what leads to a reduced trace metal input in recent years [19], [20].

VI. Conclusion

This study investigated gradual changes in physically undisturbed vegetation within the Athabasca OSM region between 1984 to 2021. For this purpose, the LandTrendr algorithm was applied to a Landsat time series and three different measurement criteria were calculated from its results (Velocity V, Frequency F, and Variance S). The results were then examined in the vicinity of oil sand opencast mines, processing facilities, and SAGD mines. A major part of the vegetation in the Athabasca OSM region showed a positive development (65.9%). However, around the opencast mines in the northwest, a negative vegetation development and stability was observed, with strong disturbances noticeable up to a radius of 10 km. In the surroundings of processing facilities, the development and stability of the vegetation was disturbed within a radius of 2 km, while around SAGD mines, no effect on vegetation was detected. Thereby the analysis of the land cover classes showed that deciduous, coniferous, and mixed forests are disproportionately affected. The negative vegetation development around oil sand opencast mining and processing facilities was attributed to the input of various pollutants and trace metals emitted. Whereas the impacts of SAGD mines on vegetation are typically off-site and upstream and therefore could not be quantified in this study. Furthermore, it was evident that vegetation disturbance was most pronounced between 1990 and 2000, which eventually recovered.

This study showed the viability of assessing gradual vegetation changes using GEE with the LandTrendr algorithm, as it allows to quickly and efficiently work on large areas and long time series. Future research should continue to analyze vegetation disturbances resulting from oil sand mining operations, especially SAGD mines.

Acknowledgment

The authors would like to thank Deutsche Forschungsgemeinschaft (DFG) and Open Access Publishing Fund of Osnabrück University.

References

[1] J. Kurek, J. L. Kirk, D. C. G. Muir, X. Wang, M. S. Evans, and J. P. Smol, "Legacy of a half century of Athabasca oil sands development recorded by lake ecosystems," *Proc. Nat. Acad. Sci.*, vol. 110, no. 5, pp. 1761–1766, Jan. 2013.

[2] J. Czarnecki, B. Radoev, L. L. Schramm, and R. Slavchev, "On the nature of Athabasca oil sands," *Adv. Colloid Interface Sci.*, vol. 114–115, pp. 53–60, Jun. 2005.

[3] S. M. Jordaan, "Land and water impacts of oil sands production in Alberta," *Environ. Sci. Technol.*, vol. 46, no. 7, pp. 3611–3617, Apr. 2012.

[4] D. Pouliot and R. Latifovic, "Land change attribution based on landsat time series and integration of ancillary disturbance data in the Athabasca oil sands region of Canada," *GISci. Remote Sens.*, vol. 53, no. 3, pp. 382–401, May 2016.

[5] J. Verbesselt, R. Hyndman, G. Newnham, and D. Culvenor, "Detecting trend and seasonal changes in satellite image time series," *Remote Sens. Environ.*, vol. 114, no. 1, pp. 106–115, Jan. 2010.

[6] C. G. Diniz et al., "DETER-B: The new amazon near real-time deforestation detection system," *IEEE J. Sel. Topics Appl. Earth Observ. Remote Sens.*, vol. 8, no. 7, pp. 3619–3628, Jul. 2015.

[7] J. Hu and Y. Zhang, "Seasonal change of land-use/land-cover (LULC) detection using modis data in rapid urbanization regions: A case study of the pearl river delta region (China)," *IEEE J. Sel. Topics Appl. Earth Observ. Remote Sens.*, vol. 6, no. 4, pp. 1913–1920, Aug. 2013.

[8] J. E. Vogelmann, A. L. Gallant, H. Shi, and Z. Zhu, "Perspectives on monitoring gradual change across the continuity of landsat sensors using time-series data," *Remote Sens. Environ.*, vol. 185, pp. 258–270, Nov. 2016.

[9] L. Ye, M. Liu, X. Liu, and L. Zhu, "Developing a new disturbance index for tracking gradual change of forest ecosystems in the hilly red soil region of southern China using dense landsat time series," *Ecological Informat.*, vol. 61, Mar. 2021, Art. no. 101221.

[10] Government of Canada, "Oil sands: Land use and reclamation," 2022, Accessed: Jan. 2, 2022. [Online]. Available: https://www.nrcan.gc.ca/energy/publications/18740

[11] D. B. D. Simmons and J. P. Sherry, "Plasma proteome profiles of white sucker (catostomus commersonii) from the Athabasca river within the oil sands deposit," *Comp. Biochem. Physiol. Part D: Genomic. Proteomic.*, vol. 19, pp. 181–189, Sep. 2016.

[12] C. M. Godwin, R. M. R. Barclay, and J. E. G. Smits, "Tree swallow (tachycineta bicolor) nest success and nestling growth near oil sands mining operations in northeastern Alberta, Canada," *Can. J. Zool.*, vol. 97, no. 6, pp. 547–557, Jun. 2019.

[13] M. M. Lynam, J. T. Dvonch, J. A. Barres, M. Morishita, A. Legge, and K. Percy, "Oil sands development and its impact on atmospheric wet deposition of air pollutants to the Athabasca oil sands region, alberta, Canada," *Environ. Pollut.*, vol. 206, pp. 469–478, Nov. 2015.

[14] E. N. Kelly et al., "Oil sands development contributes polycyclic aromatic compounds to the Athabasca river and its tributaries," *Proc. Nat. Acad. Sci.*, vol. 106, no. 52, pp. 22346–22351, Dec. 2009.

[15] M. Evans et al., "PAH distributions in sediments in the oil sands monitoring area and western lake Athabasca: Concentration, composition and diagnostic ratios," *Environ. Pollut.*, vol. 213, pp. 671–687, Jun. 2016.

[16] S. F. Bartels, B. Gendreau-Berthiaume, and S. E. Macdonald, "The impact of atmospheric acid deposition on tree growth and forest understory vegetation in the Athabasca oil sands region," *Sci. Total Environ.*, vol. 696, 2019, Art. no. 133877.

[17] C. J. Davidson, K. R. Foster, and R. N. Tanna, "Forest health effects due to atmospheric deposition: Findings from long-term forest health monitoring in the Athabasca oil sands region," *Sci. Total Environ.*, vol. 699, Jan. 2020, Art. no. 134277.

[18] B. C. Proemse, D. G. Maynard, and B. Mayer, "Foliage chemistry of Pinus banksiana in the Athabasca oil sands region, alberta, Canada," *Forests*, vol. 7, no. 12, Dec. 2016, Art. no. 312. [Online]. Available: https://www.mdpi.com/1999-4907/7/12/312

[19] Y. Gopalapillai et al., "Source analysis of pollutant elements in winter air deposition in the athabasca oil sands region: A temporal and spatial study," *ACS Earth Space Chem.*, vol. 3, no. 8, pp. 1656–1668, Aug. 2019.

[20] C. A. Cooke et al., "Spatial and temporal patterns in trace element deposition to lakes in the Athabasca oil sands region (alberta, Canada)," *Environ. Res. Lett.*, vol. 12, no. 12, Dec. 2017, Art. no. 124001.

[21] K. M. Eccles, B. D. Pauli, and H. M. Chan, "The use of geographic information systems for spatial ecological risk assessments: An example from the Athabasca oil sands area in Canada," *Environ. Toxicol. Chem.*, vol. 38, no. 12, pp. 2797–2810, Dec. 2019.

[22] R. Latifovic, K. Fytas, J. Chen, and J. Paraszczak, "Assessing land cover change resulting from large surface mining development," *Int. J. Appl. Earth Observ. Geoinformation*, vol. 7, no. 1, pp. 29–48, May 2005.

[23] S. N. Gillanders, N. C. Coops, M. A. Wulder, and N. R. Goodwin, "Application of landsat satellite imagery to monitor land-cover changes at the Athabasca oil sands, Alberta, Canada," *Can. Geographer / Le Géographe Canadien*, vol. 52, no. 4, pp. 466–485, 2008.

[24] R. Latifovic and D. Pouliot, "Monitoring cumulative long-term vegetation changes over the Athabasca oil sands region," *IEEE J. Sel. Topics Appl. Earth Observ. Remote Sens.*, vol. 7, no. 8, pp. 3380–3392, Aug. 2014.

[25] T. Kim and H. Han, "Analysis of surface displacement of oil sands region in Alberta, Canada using sentinel-1 sar time series images," *Korean J. Remote Sens.*, vol. 38, no. 2, pp. 139–151, Apr. 2022.

[26] R. Touzi, K. Omari, B. Sleep, and X. Jiao, "Scattered and received wave polarization optimization for enhanced peatland classification and fire damage assessment using polarimetric palsar," *IEEE J. Sel. Topics Appl. Earth Observ. Remote Sens.*, vol. 11, no. 11, pp. 4452–4477, Nov. 2018.

[27] Oil Sands Monitoring Program, "Oil sands monitoring program: Annual Report for 2018-19," 2018. Accessed: Nov. 18, 2021. [Online]. Available: https://open.alberta.ca/publications/2562-9182

[28] N. Gorelick, M. Hancher, M. Dixon, S. Ilyushchenko, D. Thau, and R. Moore, "Google earth engine: Planetary-scale geospatial analysis for everyone," *Remote Sens. Environ.*, vol. 202, pp. 18–27, Dec. 2017.

[29] R. E. Kennedy et al., "Implementation of the LandTrendr algorithm on google earth engine," *Remote Sens.*, vol. 10, no. 5, May 2018, Art. no. 691.

[30] S. L. Strilesky, E. R. Humphreys, and S. K. Carey, "Forest water use in the initial stages of reclamation in the athabasca oil sands region," *Hydrological Processes*, vol. 31, no. 15, pp. 2781–2792, Jul. 2017.

[31] K. Devito, C. Mendoza, and C. Qualizza, "Conceptualizing water movement in the boreal plains. implications for watershed reconstruction," p. 164, 2012, Accessed: Mar. 23, 2022. [Online]. Available: https://era.library.ualberta.ca/items/d934019b-141c-4da4-8495-cb634e6f75cf/view/c2812790-b1e0-44be-9f9e-bae6472640ae/DevitoMendozaQualizza_2012_Synthesis-Boreal-Plain-Hydrology-for-Oil-Sand-Reconstruction.pdf

[32] O. Volik et al., "Wetlands in the Athabasca oil sands region: The nexus between wetland hydrological function and resource extraction," *Environ. Rev.*, vol. 28, no. 3, pp. 246–261, Sep. 2020.

[33] J. M. Culp, R. B. Brua, E. Luiker, and N. E. Glozier, "Ecological causal assessment of benthic condition in the oil sands region, athabasca river, Canada," *Sci. Total Environ.*, vol. 749, Dec. 2020, Art. no. 141393.

[34] J. L. Kirk et al., "Atmospheric deposition of mercury and methylmercury to landscapes and waterbodies of the Athabasca oil sands region," *Environ. Sci. Technol.*, vol. 48, no. 13, pp. 7374–7383, Jul. 2014.

[35] J. Zhou, H. Li, L. Zhao, and R. Chow, "Role of mineral flotation technology in improving bitumen extraction from mined athabasca oil sands: I flotation chemistry of water-based oil sand extraction," *Can. J. Chem. Eng.*, vol. 96, no. 9, pp. 1986–1999, Sep. 2018.

[36] A. B. M. Institute and A. H. F. M. Program, "Wall-to-wall human footprint inventory enhanced for the oil sands region," 2021, Accessed: Dec. 5, 2021. [Online]. Available: https://www.abmi.ca/home/data-analytics/da-top/da-product-overview/Human-Footprint-Products/HF-inventory.html

[37] B. C. Bright, A. T. Hudak, R. E. Kennedy, J. D. Braaten, and A. H. Khalyani, "Examining post-fire vegetation recovery with landsat time series analysis in three western north american forest types," *Fire Ecol.*, vol. 15, no. 8, pp. 1–14, Apr. 2019.

[38] T. Hermosilla, M. A. Wulder, J. C. White, and N. C. Coops, "Land cover classification in an era of big and open data: Optimizing localized implementation and training data selection to improve mapping outcomes," *Remote Sens. Environ.*, vol. 268, Jan. 2022, Art. no. 112780.

[39] D. Roy et al., "Characterization of landsat-7 to landsat-8 reflective wavelength and normalized difference vegetation index continuity," *Remote Sens. Environ.*, vol. 185, pp. 57–70, Nov. 2016.

[40] Z. Zhu, S. Wang, and C. E. Woodcock, "Improvement and expansion of the fmask algorithm: Cloud, cloud shadow, and snow detection for landsats 4–7, 8, and sentinel 2 images," *Remote Sens. Environ.*, vol. 159, pp. 269–277, Mar. 2015.

[41] L. Gao et al., "Remote sensing algorithms for estimation of fractional vegetation cover using pure vegetation index values: A review," *Photogrammetry Remote Sens.*, vol. 159, pp. 364–377, Jan. 2020.

[42] R. E. Kennedy, Z. Yang, and W. B. Cohen, "Detecting trends in forest disturbance and recovery using yearly landsat time series: 1. LandTrendr - Temporal segmentation algorithms," *Remote Sens. Environ.*, vol. 114, no. 12, pp. 2897–2910, Dec. 2010.

[43] W. B. Cohen and S. N. Goward, "Landsat's role in ecological applications of remote sensing," *BioScience*, vol. 54, no. 6, pp. 535–545, Jun. 2004.

[44] J. Vogelmann, "Comparison between 2 vegetation indexes for measuring different types of forest damage in the north-eastern united-states," *Int. J. Remote Sens.*, vol. 11, no. 12, pp. 2281–2297, Dec. 1990.

[45] A. Cocke, P. Fule, and J. Crouse, "Comparison of burn severity assessments using differenced normalized burn ratio and ground data," *Int. J. Wildland Fire*, vol. 14, no. 2, pp. 189–198, 2005.

[46] S. Liu, X. Wei, D. Li, and D. Lu, "Examining forest disturbance and recovery in the subtropical forest region of Zhejiang province using landsat time-series data," *Remote Sens.*, vol. 9, no. 5, May 2017, Art. no. 479.

[47] P. Griffiths et al., "Forest disturbances, forest recovery, and changes in forest types across the carpathian ecoregion from 1985 to 2010 based on landsat image composites," *Remote Sens. Environ.*, vol. 151, no. SI, pp. 72–88, Aug. 2014.

[48] R. Seidl, W. Rammer, and T. A. Spies, "Disturbance legacies increase the resilience of forest ecosystem structure, composition, and functioning," *Ecol. Appl.*, vol. 24, no. 8, pp. 2063–2077, Dec. 2014.

[49] S. Khanna, M. J. Santos, S. L. Ustin, and P. J. Haverkamp, "An integrated approach to a biophysiologically based classification of floating aquatic macrophytes," *Int. J. Remote Sens.*, vol. 32, no. 4, pp. 1067–1094, 2011.

[50] E. A. Bolch et al., "Remote detection of invasive alien species," pp. 267–307, 2020, doi: 10.1007/978-3-030-33157-3_12.

[51] S. M. Jordaan, D. W. Keith, and B. Stelfox, "Quantifying land use of oil sands production: A life cycle perspective," *Environ. Res. Lett.*, vol. 4, no. 2, Apr.–Jun. 2009, Art. no. 024004.

[52] S. A. Watmough, A. Bird, A. Mcdonough, and E. Grimm, "Forest fertilization associated with oil sands emissions," *Ecosystems*, vol. 22, no. 1, pp. 1–14, 2018.

[53] J. Jautzy, J. M. E. Ahad, C. Gobeil, and M. M. Savard, "Century-long source apportionment of pAHs in Athabasca oil sands region lakes using diagnostic ratios and compound-specific carbon isotope signatures," *Environ. Sci. Technol.*, vol. 47, no. 12, pp. 6155–6163, Jun. 2013.

[54] C. Boutin and D. Carpenter, "Assessment of wetland/upland vegetation communities and evaluation of soil-plant contamination by polycyclic aromatic hydrocarbons and trace metals in regions near oil sands mining in alberta," *Sci. Total Environ.*, vol. 576, pp. 829–839, Jan. 2017.

[55] W. Shotyk et al., "Dust is the dominant source of "heavy metals" to peat moss (sphagnum fuscum) in the bogs of the Athabasca bituminous sands region of northern Alberta," *Environ. Int.*, vol. 92–93, pp. 494–506, Jul./Aug. 2016.

[56] R. A. Frank et al., "Profiling oil sands mixtures from industrial developments and natural groundwaters for source identification," *Environ. Sci. Technol.*, vol. 48, no. 5, pp. 2660–2670, Mar. 2014.

[57] D. M. Brown, G. W. Reuter, and T. K. Flesch, "Temperature, precipitation, and lightning modification in the vicinity of the Athabasca oil sands," *Earth Interact.*, vol. 15, no. 32, pp. 1–14, Dec. 2011.

[58] J. Pearse, V. Singhroy, S. Samsonov, and J. H. Li, "Anomalous surface heave induced by enhanced oil recovery in northern Alberta: Insar observations and numerical modeling," *J. Geophys. Res.-Solid Earth*, vol. 119, no. 8, pp. 6630–6649, 2014.

[59] A. Hossini, V. Mostafavi, and D. Bresee, "Investigation of post-abandonment surface subsidence in steam-assisted-gravity-drainage operations," *SPE Reservoir Eval. Eng.*, vol. 21, no. 3, pp. 772–788, 2018.

Moritz Lucas received the B.A. degree in geography from the University of Bremen, Bremen, Germany, in 2020. He is currently working toward the M.Sc. degree in geoinformatics with the University of Osnabrück, Osnabrück, Germany.

Besides, he works as a Working Student with Osnabrück University–Working Group Remote Sensing and Digital Image Analysis. His research interests include machine and deep learning, change analysis and forest monitoring.

Antara Dasgupta received the M.Sc. degree in remote sensing and GIS from the Faculty of Earth Observation and Geoinformation Science, ITC, University of Twente, Enschede, The Netherlands, in 2015, and the Ph.D. degree in civil engineering from the Indian Institute of Technology Bombay, Mumbai, India, and Monash University, Clayton VIC, Australia, in 2020.

She was the Senior Radar Scientist at Cloud to Street until 2021, when she joined the University of Osnabrueck as a Postdoctoral Research Assistant. Since 2018, she has served as a Reviewer for multiple international journals including IEEE TGRS, IEEE GRSL, and IEEE JSTARS.

Björn Waske (Member, IEEE) received the degree in applied environmental sciences with a major in remote sensing from Trier University, Trier, Germany, in 2002, and the Ph.D. degree in geography from the University of Bonn, Bonn, Germany, in 2007.

He was a Postdoctoral Researcher with the Faculty of Electrical and Computer Engineering, University of Iceland, Reyjavik, Iceland, from 2008 to 2009. He was a Professor of remote sensing with the University of Bonn, Bonn, Germany, until 2013 and with the Freie Universität Berlin, Germany, until 2018. Since then, he has been a Professor of remote sensing and digital image analysis with University of Osnabrück, Osnabrück, Germany.

Prof. Waske is an Associate Editor for IEEE JSTARS and reviewer for different international journals, including the IEEE TGRS, IEEE GRSL, and IEEE JSTARS.